Observation of stimulated Mie-Bragg scattering from large-size-gold-nanorod suspension in water

Guang S. He, Ken-Tye Yong, Jing Zhu, and P. N. Prasad
The Institute for Lasers, Photonics and Biophotonics, State University of New York at Buffalo, Buffalo, New York 14260-3000, USA
(Received 4 January 2011; published 24 April 2012)

Highly directional backward stimulated scattering has been observed from large-size-gold nanorods suspended in water, pumped with ~816 nm and ~10 ns laser pulses. In comparison with other known stimulated scattering effects, the newly observed effect exhibits the following features. (i) The scattering centers are impurity particles with a size comparable in order of magnitude to the incident wavelength. (ii) There is no frequency shift between the pump wavelength and the stimulated scattering wavelength. (iii) The pump threshold can be significantly lower than that of stimulated Brillouin scattering in pure water. The nonfrequency shift can be explained by the formation of a standing-wave Bragg grating induced by the interference between the forward pump beam and the backward Mie-scattering beam. The low pump threshold results from stronger initial Mie-scattering (seed) signals and the intensity-dependent refractive-index change of the scattering medium enhanced by metallic nanoparticles.

DOI: 10.1103/PhysRevA.85.043839 PACS number(s): 42.65.Es, 42.90.+m

I. INTRODUCTION

Stimulated scattering of intense coherent light is one of the important research subjects in the areas of quantum electronics and nonlinear optics [1,2]. So far, several different types of stimulated scattering effects have been reported, mainly including stimulated Raman scattering (SRS) [3], stimulated Brillouin scattering (SBS) [4], stimulated Rayleigh-wing scattering (SRWS) [5], stimulated thermal Rayleigh scattering (STRS) [6,7], stimulated Kerr scattering (SKS) [8,9], as well as stimulated Rayleigh-Bragg scattering (SRBS) [10,11]. For all of these known effects, the scattering centers are always the atoms or molecules of a homogeneous scattering medium.

On the other hand, in nature and daily life, there is another type of scattering phenomenon, which is the scattering from impurity particles or external micro-objects suspended in a homogeneous neat medium; the most familiar examples are the scattering from clouds in air and from milk in water. This type of conventional scattering is generally called Mie scattering [12–14], of which the wavelength dependence of the scattering cross section is mainly determined by the ratio of the particle size to the incident wavelength for a given refractive index difference between the particle and the surrounding homogeneous medium.

For a long time, researchers rarely thought of the possibility of generating stimulated scattering from those impurity particles. However, the recent development of nanotechnology has brought a new opportunity for conducting thorough studies on the scattering properties of semiconductor and metal nanoparticle systems. Among them, Au nanoparticles of various shapes and sizes dispersed in water are employed for fundamental research because of their high stability, good optical quality, and ease of preparation [15]. El-Sayed *et al*. have performed systematic studies on the extinction spectra of Au nanorods in water, specifically establishing the relationship between the characteristic extinction spectral bands and the aspect ratio of the Au nanorods [16]. They also presented some computation results of the Mie-scattering contribution to the overall (absorption plus scattering) extinction by using Mie theory and modified numerical methods [17]. In the meantime, some experimental results of scattering measurements on metal nanoparticles have been reported [18,19].

In this work, we report that under appropriate pump conditions a highly directional backward stimulated scattering can be effectively generated in a Au-nanorod system suspended in water. In comparison with other known types of stimulated scattering, the newly observed effect exhibits the features of no frequency shift and low pump threshold requirement. To explain the experimental results and the above features, a gain mechanism of induced Bragg grating reflection is proposed.

II. SCATTERING MEDIUM AND EXPERIMENTAL SETUP

In our stimulated scattering experiment, the scattering centers are gold nanorods of ~13 nm diameter and ~90 nm length; their transmission-electron-microscope (TEM) image is shown in Fig. 1(a), while the transmission spectra of their suspension in water with 37 mg/mL concentration (1.6×10^{14} cm^{-3} particle density) and two different path lengths are shown in Fig. 1(b). The gold nanorods were prepared by the method described by Nikoobakht *et al*. [20].

From Fig. 1(b) we can see that there are two major linear extinction bands: one is in ~530 nm wavelength position and the other is in ~1100 nm position. These two extinction bands are caused by the surface-plasmon resonance along the shorter dimension and longer dimension of the nanorods, respectively [15,16]. Note that the measured extinction spectra contain two contributions: absorption and scattering. The general rules for generating stimulated scattering are (i) a lower linear absorption loss and (ii) a large initial spontaneous scattering signal. According to the first requirement, the pump wavelength should be in an ~800 nm range, where the minimum extinction is located. To consider the second requirement, we have to separate the scattering extinction from the overall extinction. Based on our recent study, the scattering extinction spectra of a Au-nanorod system can be separated from the overall extinction spectra. As an example, Fig. 2(a) shows the measured overall extinction spectral curve and the scattering extinction curve of the Au nanorods (~10.5 nm in diameter and ~75 nm in length) in water [21]. The normalized peak value of the scattering extinction coefficient is about 1/30 of that of the overall extinction, while the scattering coefficient values in the gap range between those two extinction bands

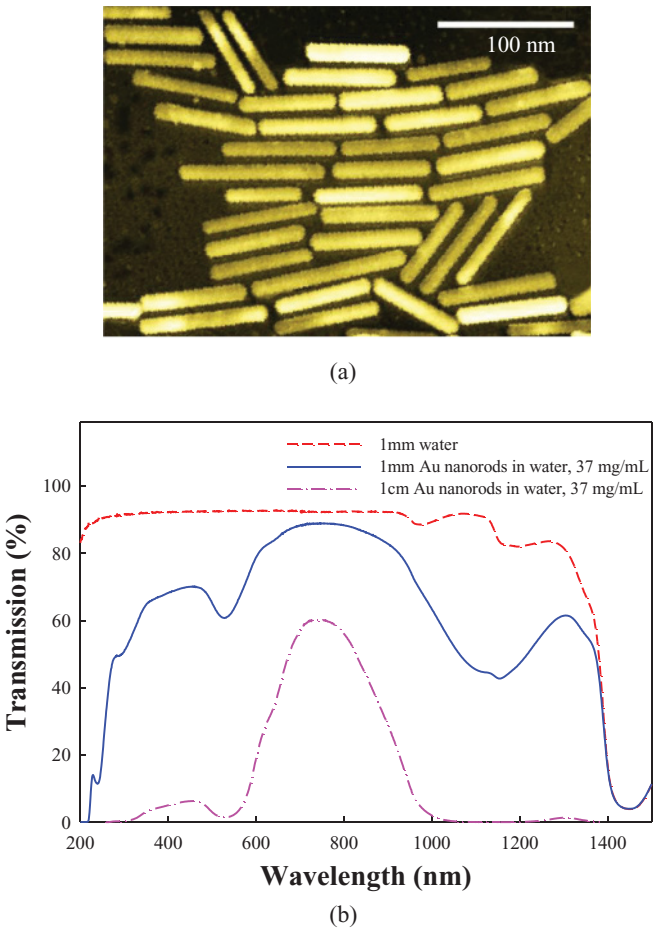

FIG. 1. (Color online) (a) TEM image of Au nanorods used for stimulated scattering experiment; (b) transmission spectra for 1 mm water sample and 1 mm and 1 cm Au-nanorod–water samples.

remain comparable to those in the band ranges. This example implies that from Au-nanorod suspension systems one may achieve a much larger spontaneous Mie-scattering (seed) signal while retaining an acceptable absorption loss by choosing a suitable pump wavelength and sample concentration. For the 1 cm Au-nanorod–water sample shown in Fig. 1(b), the 90° Mie-scattering intensity measured by using an ~800 nm pulsed laser beam was about three orders of magnitude stronger than Rayleigh scattering from a 1 cm pure water sample.

Shown in Fig. 2(b) is the measured angular dependence of scattering intensity from an Au-nanorod–water sample (with a nanorod diameter of ~16 nm and length of ~65 nm), which was obtained by using an unfocused 778 nm pulsed laser as the incident light linearly polarized along a 45° direction with the observation plane [21]. By contrast, Fig. 2(c) shows the calculated curve based on Rayleigh-scattering theory. On the one hand, from Fig. 2(a) one can see that the spectral distribution of scattering from Au nanorods is entirely different from that predicted by Rayleigh-scattering theory (simple $1/\lambda^4$ relation). Comparing Fig. 2(b) to 2(c), one can see that the angular distribution of scattering from the Au-nanorod–water sample also significantly deviates from the prediction of Rayleigh theory based on assumption of pointlike scatters.

As an example of comparison between the Rayleigh scattering from a pure water sample and Mie scattering from a Au-nanorod–water sample, Fig. 3 shows the side view of a laser-beam-induced scattering appearance from these two samples. The incident laser beams have nearly the same ~10 ns pulse duration and energy but with three different wavelengths, i.e., 408, 532, and 816 nm, respectively. From Fig. 3 one can easily see that the Rayleigh scattering from the water cell becomes much weaker as the wavelength of the input beam gets longer, whereas the Mie scattering is always much stronger than the former.

The pump source for generating stimulated scattering was a tunable dye laser system pumped by a frequency-doubled Q-switched Nd:YAG (yttrium aluminum garnet) laser (PR-230-10 from Spectra-Physics). This dye laser system provided an output of ~816 nm wavelength, ~0.022 nm spectral linewidth, ~10 ns pulse duration, ~0.36 mrad beam divergence, and 10 Hz repetition rate. This dye laser pump beam was linearly polarized and its pulse energy could be varied from 10 μJ to 6 mJ by rotating a prism polarizer. The pump beam was focused via an $f = 15$ cm lens onto the center of a 2-cm-long cuvette containing the sample of Au nanorods (~13 nm in diameter and ~90 nm in length) in water of 37 mg/mL concentration. In order to avoid the reflection influence from the two optical windows of the cuvette, the incident angle of the pump beam was kept in a 5°–10° range.

III. PROPERTIES OF BACKWARD STIMULATED SCATTERING

Under the experimental conditions mentioned above, once the pump energy (intensity) exceeds a certain threshold value, a highly directional backward stimulated scattering beam can be observed. This measured pump energy (or intensity) threshold value was ~0.5 mJ (or ~2.2 GW/cm^2).

Shown in Fig. 4 are the photographs of the spectral lines for the pump beam alone (b), for the backward stimulated scattering beam alone (d), and for the two beams together (c). These spectral lines are measured by a 1 m two-grating spectrograph (ISA from Jobin Yvon) in conjunction with a CCD-array detector (EDC-1000E from Electrim). The apparatus linewidth of the spectrograph system was calibrated by using the 532 nm laser line from the same frequency-doubled Nd:YAG laser operating in a single axial mode. As shown in Fig. 4(a), the measured apparatus linewidth (FWHM) at an ~532 nm range is $\delta\lambda \approx 0.0058$ nm, and the estimated apparatus linewidth at an ~816 nm range should be $\delta\lambda' \approx 0.0089$ nm. To obtain the photos shown in Figs. 4(b)–4(d), the pump beam and the backward stimulated scattering beam were incident with slightly shifted positions on the entrance slit of the spectrograph. Under such arrangements, the spectral lines of these two beams were separated vertically from each other, and the spectral resolution of wavelength-shift measurement should be $\delta\lambda'/2 \approx 0.0045$ nm at an ~816 nm range. As shown in Fig. 4(c), there is no wavelength shift between the pump line and stimulated scattering line, with a spectral resolution much narrower than the half of the pump linewidth.

Shown in Fig. 5 are the temporal waveforms of the pump pulse and stimulated scattering pulse, measured at different pump energy levels by using a 500 MHz dual channel

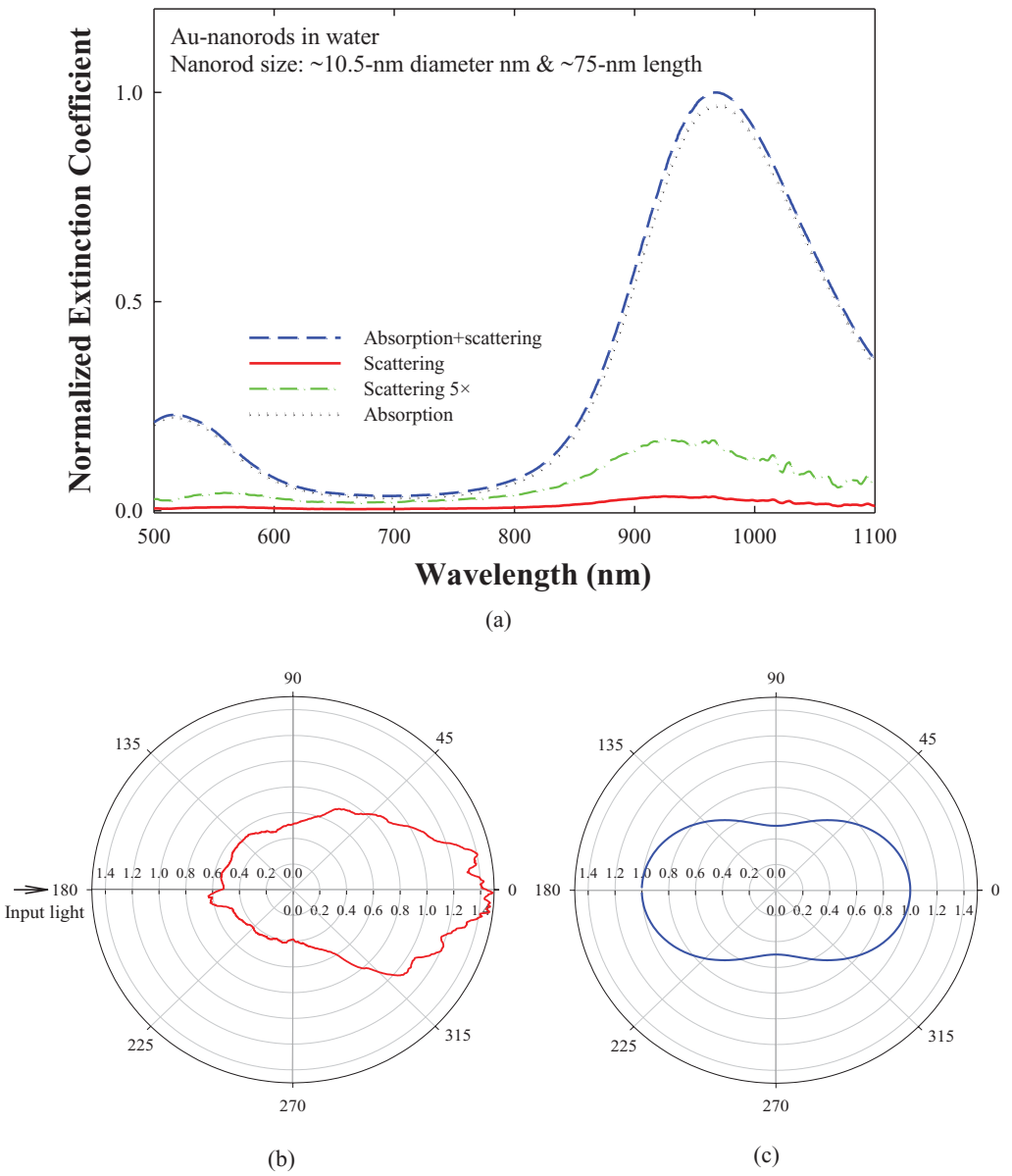

FIG. 2. (Color online) (a) Measured normalized overall extinction coefficient (dashed line) and scattering coefficient (solid line) of an Au-nanorod–water sample as a function of wavelength. (b) Measured normalized angular dependence of scattering from an Au-nanorod–water sample (nanorod diameter ~16 nm, length ~65 nm); the 778 nm incident light was linearly polarized along a 45° direction with the observation plane. (c) Calculated curve based on Rayleigh scattering theory.

oscilloscope (Infinum from HP) in conjunction with two identical photodiodes with a 1 ns resolution. From this figure, one can see that the duration of the stimulated scattering pulse is always shorter than that of the corresponding pump pulse. This is understandable by considering the threshold requirement for pump intensity that is a function of time.

Figure 6 shows the measured far-field patterns for the pump beam and the stimulated scattering beam by using an $f =$ 100 cm focusing lens and a CCD-array detector placed in the focal plane position, indicating that the divergence angle (0.22 mrad) of the backward stimulated scattering beam is smaller than that (0.36 mrad) of the input pump beam. This feature can be explained by considering the threshold requirement for the local pump intensity of a focused pump beam with a quasi-Gaussian transverse intensity distribution.

Moreover, the measured backward stimulated scattering energy as a function of the input pump energy is shown in Fig. 7 for the two sample solutions with different concentration values. From the measured data, we can see that at the same pump energy level, the sample solution with a higher concentration can provide a greater output stimulated scattering energy. The energy conversion efficiency from the pump pulse to the stimulated scattering pulse is higher than 15% for the high-concentration sample at the pump energy levels of 3.5–4 mJ.

It is experimentally shown that the pump energy (intensity) threshold for generating stimulated scattering becomes higher when the sample solution's concentration value is decreased. The measured threshold values for three different concentration values are presented in Table I.

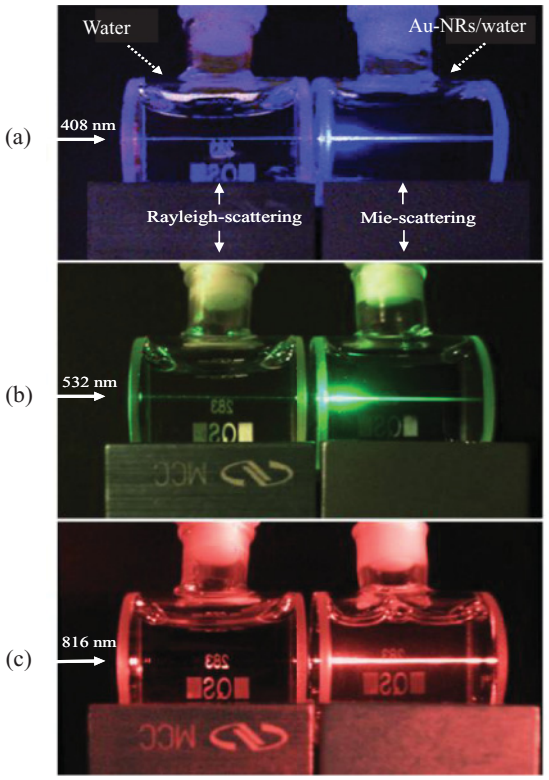

FIG. 3. (Color online) Laser-beam-induced Rayleigh scattering in water (left cell) and Mie scattering in Au nanorods (right cell): (a) incident wavelength 408 nm, (b) incident wavelength 532 nm, and (c) incident wavelength 816 nm. Laser pulse duration: ∼10 ns.

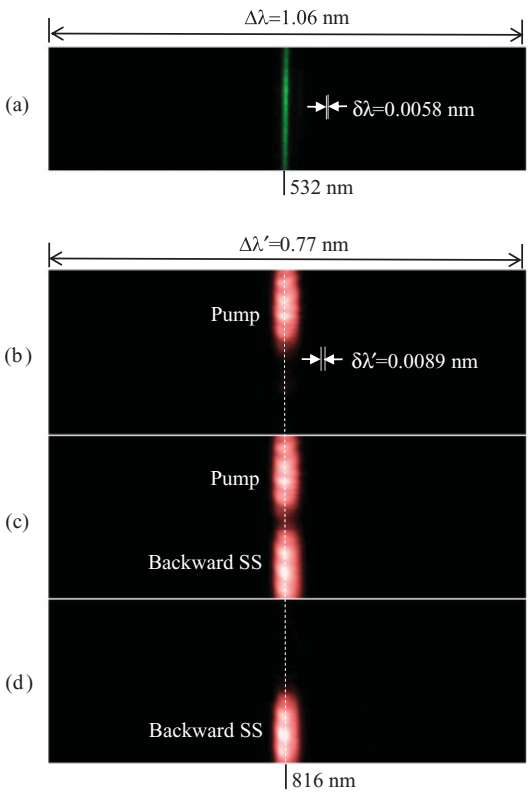

FIG. 4. (Color online) Spectrograms for (a) the 532 nm line of the laser beam from a single axial-mode frequency-doubled Nd:YAG laser, (b) the 816 nm line of the pump beam alone, (c) the spectral lines of both pump and backward stimulated scattering (SS) beams, and (d) the spectral line of the SS beam alone. $\delta\lambda$ and $\delta\lambda'$ indicate the apparatus linewidth values in 532 nm range and in 816 nm range, respectively. All photos are taken on a single-pulse exposure.

To explore the origin of the observed effect, the possibility of STRS or stimulated thermal Brillouin scattering (STBS) should be considered, because there is relatively large residual linear absorption at the pump wavelength. It is known that two special features were predicted by the theories of STRS and STBS [6,7]: (i) there would be an anti-Stokes frequency shift by the amount of half of the pump linewidth and (ii) the pump threshold of the STRS (or STBS) in an absorbing solution sample should be lower than the nonabsorbing solvent sample. First, our spectral measurement results already indicated that there is no such frequency shift; secondly, when we change the pump wavelength toward the direction of the sample's absorption peak position, the threshold requirement becomes higher. These two facts imply that the simple thermal effect is not likely responsible for the stimulated scattering reported here.

To verify the above conclusion, measurements on pump threshold among our Au-nanorod–water sample, a pure water sample, and absorbing-dye water solution samples of different linear absorption values were performed under the same 816 nm pump conditions. All samples were of the same 2 cm path length but with different absorbance values at

TABLE I. Stimulated scattering threshold measured by 816 nm and 10 ns laser pulses (Focusing length is 15 cm; sample length is 2 cm).

Scattering medium	Concentration (mg/mL)[a]	Linear transmission (1 cm length and at 816 nm)	Pump energy threshold[a] (mJ)	Pump intensity threshold (GW/cm^2)	Threshold ratio (to water)
Au-nanorod–water	37	0.58	0.5	2.22	0.19
	18	0.77	0.6	2.67	0.22
	9.0	0.88	1.0	4.44	0.37
Water		0.99	2.7	12.0	1
IR140 dye/water	6.7×10^{-4}	0.92	2.9	12.9	1.07
	1.3×10^{-3}	0.88	3.1	13.8	1.14
	2×10^{-3}	0.81	3.2	14.2	1.18
	4×10^{-3}	0.61	3.7	16.4	1.37

[a]Experimental uncertainty: ± 10%.

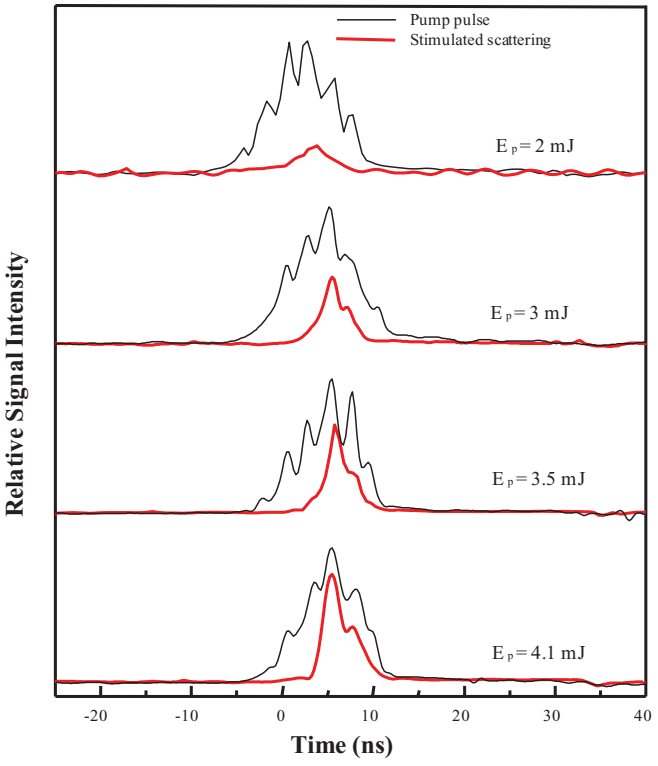

FIG. 5. (Color online) Temporal waveforms for pump pulse (thin line) and stimulated scattering pulse (thick line), measured at different pump energy levels. All waveforms are taken upon a single pulse.

the pump wavelength. As a linearly absorbing medium, the aqueous solutions of IR140 laser dye (from Exciton) with

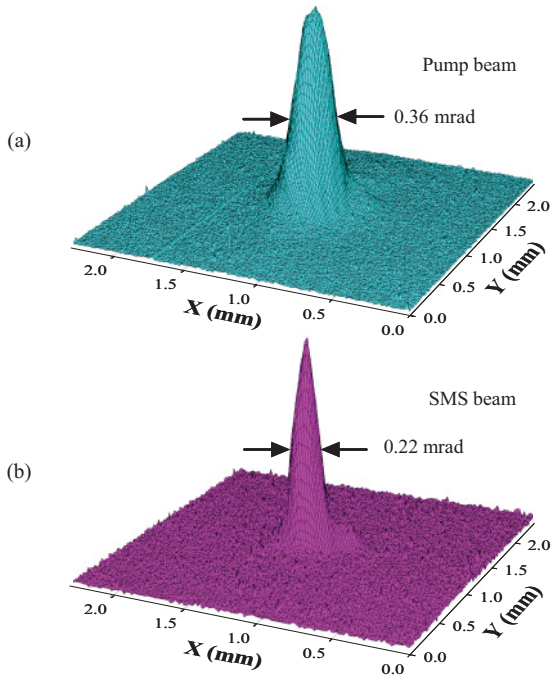

FIG. 6. (Color online) Measured far-field patterns of the pump beam (a) and backward stimulated scattering beam (b) on the focal plane of an $f = 100$ cm lens. Pump energy: 1.5 mJ.

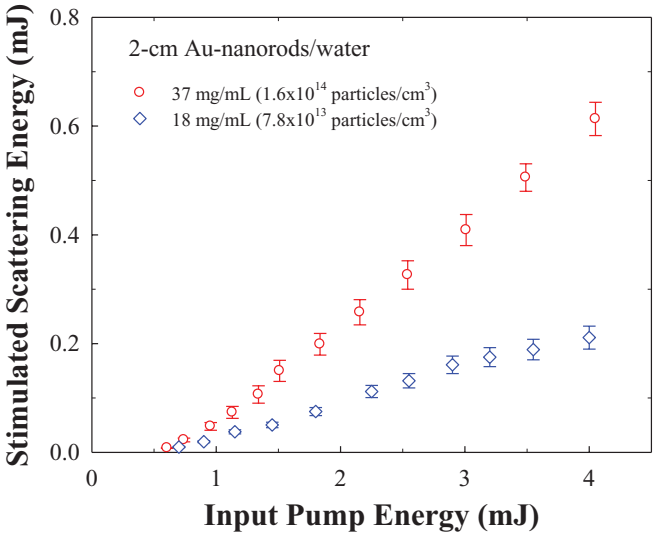

FIG. 7. (Color online) Measured backward stimulated scattering energy versus input pump energy for two Au-nanorod–water samples of different concentration values.

different concentrations were chosen for stimulated scattering experiment. The reason for choosing this dye solution to compare our Au-nanorod–water sample is that, the major absorption bands in the IR range for these two types of samples are quite similar, and the 816 nm pump wavelength is in the same side of the corresponding major absorption bands of these samples. Figure 8 shows linear transmission spectra of IR140 dye aqueous solutions with different concentration values; the linear transmission at 816 nm position varies from 0.92 to 0.61.

The measured pump threshold values for generating backward stimulated scattering in different samples are summarized in Table I. These results indicate that (i) the pump threshold for the pure water sample is five times higher than the Au-nanorod–water sample and (ii) with adding absorbing dye into the water sample, the threshold for generating stimulated scattering becomes higher following the increase of linear absorption at the pump wavelength. Based on these experimental results, we conclude that the simple heating

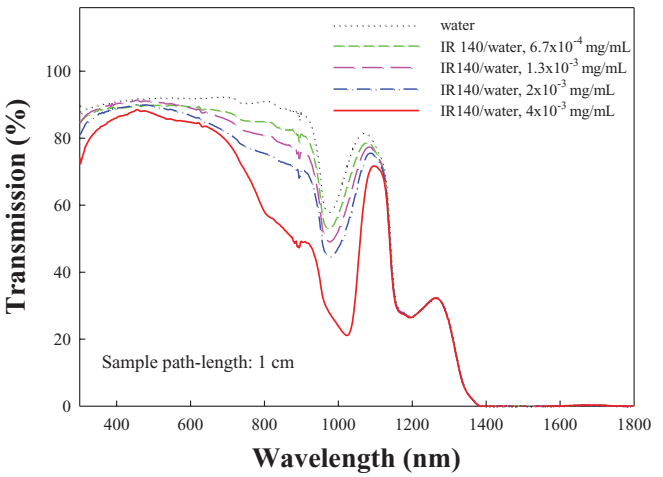

FIG. 8. (Color online) Linear transmission spectra of IR140 dye aqueous solutions with different concentration values.

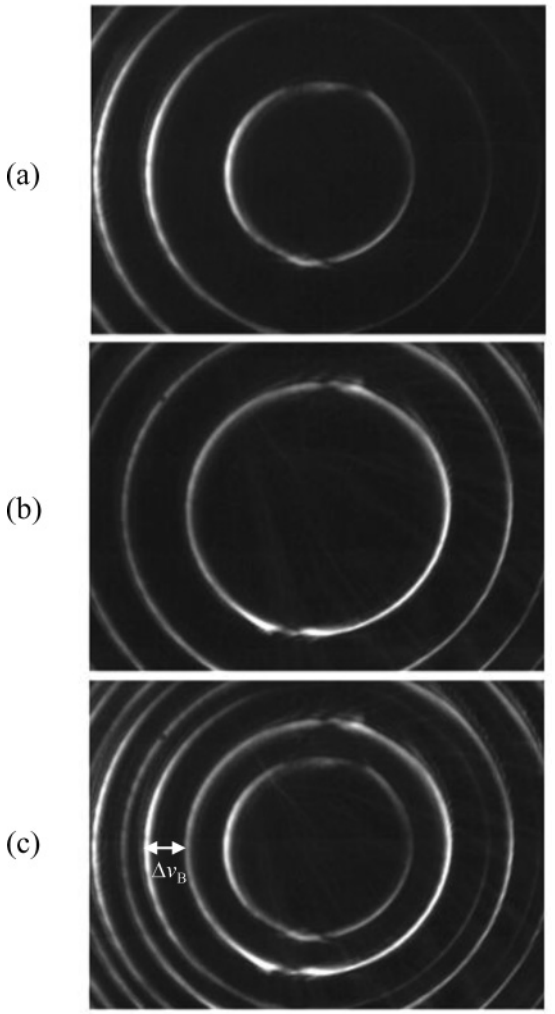

FIG. 9. Fabry-Perot interferograms of (a) partially blocked pump beam of 1064 nm, (b) stimulated Brillouin scattering beam from a pure chloroform sample, and (c) both beams together. Free spectral range is 0.43 cm^{-1}; all photos are taken by a single-pulse exposure; $\Delta\nu_B$ is the frequency shift.

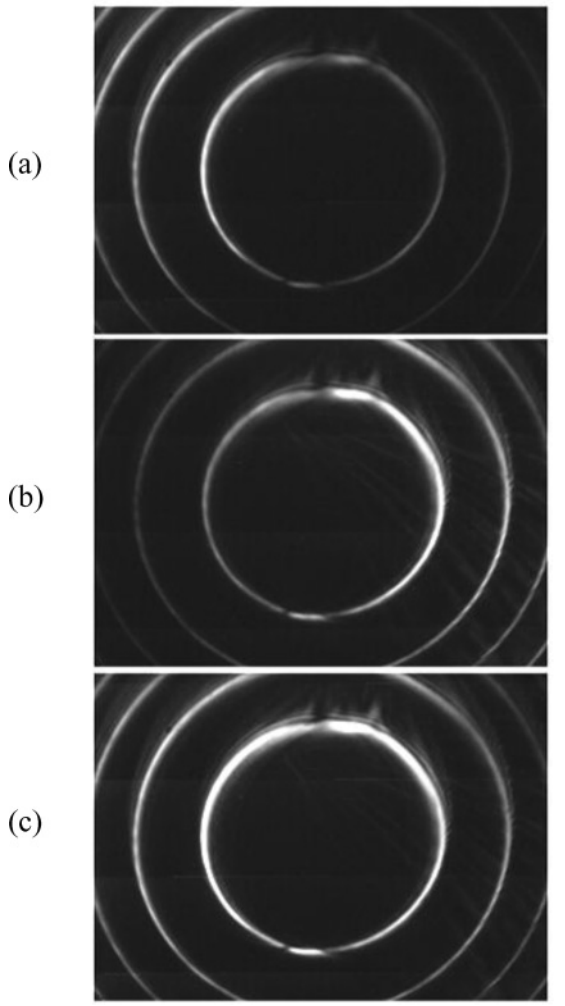

FIG. 10. Fabry-Perot interferograms of (a) partially blocked pump beam of 1064 nm, (b) stimulated Mie-scattering beam from a sample of Au -nanorods in chloroform, and (c) both beams together. Free spectral range is 0.43 cm^{-1}; all photos are taken by a single-pulse exposure, and there is no frequency shift.

effect duo to absorption cannot be the mechanism leading to the significant reduction of the pump threshold in the Au-nanorod–water sample.

Finally, to distinguish the stimulated Mie scattering (SMS) in a Au-nanorod solution from the SBS in a pure solvent, we had to use the 1064 nm pulsed output from the same Nd:YAG laser system working in a single axial mode as the pump beam with a spectral linewidth < 0.005 cm^{-1}. Since water has a considerable absorption ($\sim$12% for 1 cm path length) at that wavelength, we prefer to use the solution sample of Au nanorods in chloroform to generate SMS, and use the pure chloroform sample (with $\leqslant$0.5% absorption for 1 cm path length) for generating SBS. The spectral shift behavior is measured by a Fabry-Perot interferometer of 1.16 cm spacing in air. Shown in Fig. 9 are the recorded interferograms of the input 1064 nm pump beam (a), the SBS beam from the chloroform sample (b), and of both the beams (c), respectively. The measured SBS frequency shift for chloroform was $\Delta\nu_B \approx 0.24$ cm^{-1}. In contrast, shown in Fig. 10 are the corresponding results of SMS from the Au-nanorod–chloroform sample. We see once again that there is no frequency shift between the stimulated scattering beam and the pump beam.

IV. STIMULATED MIE-SCATTERING MODEL BASED ON INDUCED BRAGG GRATING REFLECTION

To interpret the features of no frequency shift and low pump threshold for the observed stimulated scattering in the investigated Au nanorods suspended in a solvent, we may rely on a physical model of feedback provided by an induced Bragg grating. This model has been adopted to explain the generation of stimulated Rayleigh-Bragg scattering in a multiphoton absorbing molecular medium [10,11]. According to this model and in the present case, in the beginning there is a weak backward Mie-scattering beam that can interfere with the strong forward pump beam to form a standing-wave field, as these two beams have the same frequency. Although such a standing-wave field exhibits initially small spatial intensity modulation with a period of half of the wavelength, it may lead

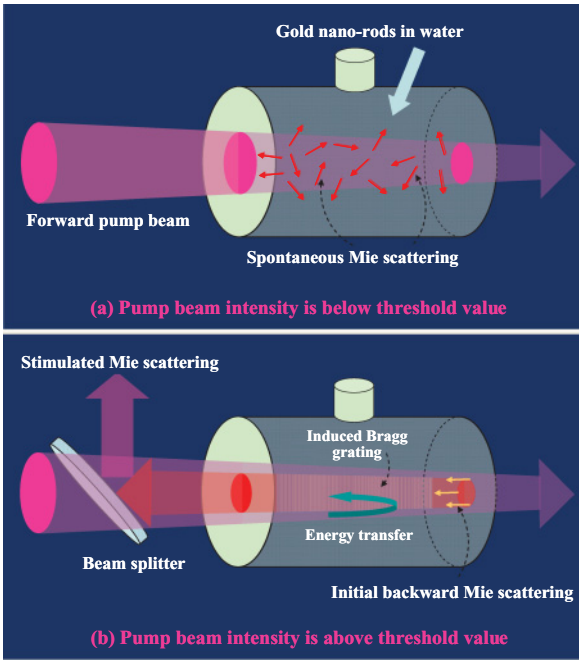

FIG. 11. (Color online) (a) Schematic diagrams showing random Mie scattering from Au nanorods in water with below-threshold pump. (b) Directional backward stimulated Mie-scattering formation with above-threshold pump.

to an induced Bragg grating via intensity-dependent refractive-index changes of the scattering medium. This grating will provide the same reflectivity to both the pump beam and the backward scattering beam. Since the former is much stronger than the latter, the net result is that the partial forward pump energy will transfer to the backward scattering beam. While the initial backward scattering beam is getting stronger, the modulation depth of the induced Bragg grating will be greater and the grating reflectivity becomes higher, which means that more pump energy will be transferred into the backward scattering beam. Here we see a typical positive feedback mechanism necessary for any type of stimulated scattering or lasing process. If the pump intensity is higher than a certain threshold level, such that the overall gain for the backward scattering beam is considerably greater than the overall loss due to various attenuation mechanisms (including absorption, side-direction scattering, and multiple scattering), the backward Mie scattering can finally become stimulated as schematically shown in Fig. 11. Here we only consider the interaction and energy transfer between the backward scattering beam and the forward pump beam, because only in this case can the effective interaction length (effective gain length) be the maximum. This same consideration is used to explain the generation of backward stimulated Brillouin scattering by using a focused pump laser beam.

Since the Bragg grating is induced by a standing-wave field consisting of the forward pump beam and the backward Mie-scattering beam, there is no frequency shift for the reflected beam from such a stationary grating. This situation is essentially different from the stimulated Brillouin scattering, where the optical feedback is based on the reflection from the induced traveling hypersonic grating due to electrostriction effect. In the latter case, there is a certain frequency shift between the stimulated scattering beam and the pump beam, owing to the Doppler effect associated with the traveling grating reflection. To distinguish from other known types of stimulated scattering effects, it is reasonable to term the newly observed effect stimulated Mie-Bragg scattering (SMBS) or simply SMS.

Assume that the pump beam propagates along the $+z$ direction through the scattering medium over length l_0, whereas the backward Mie-scattering beam propagates along the $-z$ direction. The reflectivity of the induced Bragg grating is determined by [10,11]

$$\begin{aligned} R(z) &= \tanh^2[\pi \delta n(z) l_0/\lambda_0] \\ &= \tanh^2[2\pi n_2 l_0 \sqrt{I_p(z) I_s(z)}/\lambda_0]. \end{aligned} \tag{1}$$

Here δn is the induced local refractive-index change of the scattering medium, n_2 is the nonlinear refractive-index coefficient of the scattering medium, I_p and I_s are the pump and backward scattering intensities, and λ_0 is the wavelength of both beams. Under threshold condition $R(z) \ll 1$, the hyperbolic tangent function in Eq. (1) can be replaced by its arguments, and the average reflectivity of the Bragg grating can be defined by its value at the center of the gain medium, i.e.,

$$\bar{R}_{\rm th} = (2\pi n_2 l_0/\lambda_0)^2 \bar{I}_p^{\rm th} \bar{I}_s^{\rm th}, \tag{2}$$

where

$$\begin{aligned} \bar{I}_p^{\rm th} &\approx I_p^{\rm th}(l_0/2) \approx I_p^{\rm th}(0) e^{-\alpha l_0/2}, \\ \bar{I}_s^{\rm th} &\approx I_s^{\rm th}(l_0/2) \approx \sqrt{I_s^{\rm th}(0) I_s(l_0)}. \end{aligned} \tag{3}$$

Here $I_p^{\rm th}(0)$ is the input threshold pump intensity, $I_s^{\rm th}(0)$ is the output backward stimulated scattering intensity at threshold operation, $I_s(l_0)$ is the initial backward scattering intensity, and α is the linear attenuation coefficient at λ_0. Under the threshold condition, the conservation of energy requires that

$$\bar{R}^{\rm th} \bar{I}_p^{\rm th} \geqslant I_s^{\rm th}(0). \tag{4}$$

Substituting Eqs. (2) and (3) into Eq. (4) leads to the following requirement for the threshold pump intensity:

$$\left[I_p^{\rm th}(0)\right]^2 \geqslant \left(\frac{\lambda_0}{2\pi n_2 l_0}\right)^2 e^{\alpha l_0} \sqrt{\frac{I_s^{\rm th}(0)}{I_s(l_0)}}. \tag{5}$$

Here both $I_s^{\rm th}(0)$ and $I_s(l_0)$ are the directly measurable parameters. The above condition reveals several predictions: (i) the pump threshold will be lower when the initial scattering signal $[I_s(l_0)]$ is stronger; (ii) a large n_2 value is favorable for generating stimulated scattering; and (iii) a large linear attenuation (α) is an unfavorable factor. These predictions support our experimental results. It should be noted that for Au-nanorod samples, a higher concentration is needed based on the major considerations of (i) and (ii); for linearly absorbing dye solutions, the increase of dye concentration does not help a lot for initial scattering signal and n_2 value, whereas the increased linear attenuation just simply raises the threshold values as indicated in Table I.

The same considerations can also explain why the threshold of generating stimulated scattering in the Au-nanorod–water

sample is significantly lower than the pure water sample. First, as shown in Fig. 3 the spontaneous (initial) Mie scattering is significantly stronger than the Rayleigh (or Brillouin) scattering in the water. Secondly, the contribution from the Au nanorods to the n_2 value of the scattering medium could be much greater than the pure water due to either the surface-plasmon resonance effect or the intensity-dependent redistribution effect of the Au nanoparticles in water.

However, the above-mentioned analysis is just a semiquantitative description based on a much simplified steady-state assumption. It cannot be applied to explain the dynamic details of stimulated scattering generation under the nanosecond-pulsed pump condition. For example, it cannot explain why in Fig. 5 the pulse waveform of the stimulated scattering is asymmetric on the time scale, while the waveform of the pump pulse is nearly symmetric. In a real case, the temporal responses of some involved parameters of the sample medium, such as the build-up time and relaxation time of the induced Bragg grating, should be taken into account in a more rigorous dynamic analysis [22,23], which is beyond the scope of this work.

V. CONCLUSIONS

A new type of backward stimulated scattering has been observed in a Mie-scattering medium that is Au nanorods of length comparable with incident light wavelength suspended in water, pumped by ~816 nm and ~10 ns laser pulses. This stimulated scattering features no frequency shift and much lower pump threshold requirement. The energy transfer efficient from the input pump pulse to the backward stimulated scattering pulse can be higher than 15%. A physical model of gain from induced standing-wave Bragg grating reflection is proposed, which can semiqualitatively explain the basic experimental results. The basis of Bragg grating formation is the laser-intensity-dependent refractive-index change of the scattering medium. The more specific investigation on the refractive-index change behavior in metal-nanoparticle suspension systems should be the subject of further studies.

ACKNOWLEDGMENTS

This work was supported by the U.S. Air Force Office of Scientific Research (AFOSR) through Contract No. FA9550-11-1-0121.

[1] G. S. He, in *Progress in Optics*, edited by E. Wolf (North-Holland, Amsterdam, 2009), vol. 53, pp. 201–292.
[2] W. Kaiser and M. Maier, in *Laser Handbook*, edited by F. T. Arecchi and E. O. Schulz-Dubois (North-Holland, Amsterdam, 1972), Vol. 2, pp. 1077–1150.
[3] G. Eckhardt, R. W. Hellwarth, F. J. McClung, S. E. Schwarz, D. Weiner, and E. J. Woodbury, Phys. Rev. Lett. **9**, 455 (1962).
[4] R. Y. Chiao, C. H. Townes, and B. P. Stoicheff, Phys. Rev. Lett. **12**, 592 (1962).
[5] D. I. Mash, V. V. Morozov, V. S. Starunov, and I. L. Fabelinskii, JETP Lett. **2**, 25 (1965).
[6] R. M. Herman and M. A. Gray, Phys. Rev. Lett. **19**, 824 (1967).
[7] D. H. Rank, C. W. Cho, N. D. Foltz, and T. A. Wiggings, Phys. Rev. Lett. **19**, 828 (1967).
[8] G. S. He and P. N. Prasad, Phys. Rev. A **41**, 2687 (1990).
[9] G. S. He, Y. Cui, and P. N. Prasad, JETP **85**, 850 (1997).
[10] G. S. He, T.-C. Lin, and P. N. Prasad, Opt. Express **12**, 5952 (2004).
[11] G. S. He, C. Lu, Q. Zheng, P. N. Prasad, P. Zerom, R. W. Boyd, and M. Samoc, Phys. Rev. A **71**, 063810 (2005).
[12] M. Born and E. Wolf, *The Principles of Optics* (Pergamon, New York, 1980), pp. 633–664.
[13] H. C. van de Hulst, *Light Scattering by Small Particles* (Dover, New York, 1981).
[14] C. F. Bohren and D. R. Huffman, *Absorption and Scattering of Light by Small Particles* (Wiley, New York, 1998).
[15] N. R. Jana, L. Gearheart, and C. J. Murphy, J. Phys. Chem. B **105**, 4065 (2001).
[16] S. Eustis and M. A. El-Sayed, Phys. Chem. B **109**, 16350 (2005).
[17] P. K. Jain, K. S. Lee, I. H. El-Sayed, and M. A. El-Sayed, J. Phys. Chem. B **110**, 7238 (2006).
[18] K. Aslan, P. Holley, L. Davies, J. R. Lakowicz, and C. D. Geddes, J. Am. Chem. Soc. **127**, 12115 (2005).
[19] D. D. Evanoff and G. Chumanov, J. Phys. Chem. B **108**, 13957 (2004).
[20] B. Nikoobakht and M. A. El-Sayed, Chem. Mater. **15**, 1957 (2003).
[21] G. S. He, J. Zhu, K.-T. Yong, A. Baev, H.-X. Cai, R. Hu, Y. Cui, X.-H. Zhang, and P. N. Prasad, J. Phys. Chem. C **114**, 2853 (2010).
[22] N. F. Andreev, M. A. Dvoretskiĭ, A. A. Leshchev, V. G. Manishin, G. A. Pasmanik, and T. P. Samarina, Sov. J. Quantum Electron. **15**, 928 (1985).
[23] G. C. Valley, IEEE J. Quantum Electron. **22**, 704 (1986).